



# Optimal surface roughness of Ti6Al4V alloy for the adhesion of cells with osteogenic potential

B. B. Straumal<sup>1,a)</sup>, A. S. Gornakova<sup>1</sup>, M. V. Kiselevskiy<sup>2</sup>, N. Yu. Anisimova<sup>2</sup>, A. N. Nekrasov<sup>3</sup>, A. R. Kilmametov<sup>1</sup>, R. Strug<sup>4</sup>, E. Rabkin<sup>4</sup>

<sup>1</sup>Ossipyan Institute of Solid State Physics and Scientific Center in Chernogolovka, Russian Academy of Sciences, Ac. Ossipyan str. 2, Moscow district, Chernogolovka, Russia 142432

<sup>2</sup>Laboratory of Cell Immunity "N. N. Blokhin National Medical Research Centre of Oncology" of the Health Ministry of Russia, Kashirskoe highway 23, Moscow, Russia 115 478

<sup>3</sup>Institute of Experimental Mineralogy, Russian Academy of Sciences, Ac. Ossipyan str. 4, Chernogolovka, Russia 142432

<sup>4</sup>Department of Materials Science and Engineering, Technion-Israel Institute of Technology, 3200003 Haifa, Israel

<sup>a)</sup>Address all correspondence to this author. e-mail: [straumal@issp.ac.ru](mailto:straumal@issp.ac.ru)

Received: 15 February 2022; accepted: 12 May 2022; published online: 10 June 2022

The effect of surface roughness of cold-wrought Ti-6Al-4V (VT6) alloy on the adhesion of mouse MC3T3-pre-osteoblasts cells has been studied. The array of linear grooves has been produced on the substrate surface with the aid of abrasive SiC papers with grit sizes of 220, 400, 600, 800, 1000, 1200, 2000, and 4000 (number of grains per cm<sup>2</sup>), as well as different diamond pastes with grain sizes 6, 3, and 1 μm. The grain size of this array of abrasive papers and diamond pastes monotonously decreases from 68 μm (for 220 grit paper) to 1 μm for the finest diamond paste. The adhesion of the mouse MC3T3-pre-osteoblast cells to the samples with different roughness has been measured by fluorescence microscopy. The size and morphology of adhered cells were measured by the light microscopy. The relative fraction of adhered cells behaves non-monotonously with the abrasive grain size. It is about 0.35 for grain size of 1 μm, increases up to 0.95 for grain size of 7 μm, and then slowly decreases down to 0.55 for abrasive grain size of 68 μm. The surface roughness parameters of Ti-6Al-4V (VT6) alloy correlate with the depth and width of grooves produced on the initially flat surface of the alloy. The surface ground with a grinding media corresponding to the grain size of about 10 μm exhibited highest cell adhesion. This grain size corresponding to maximum cells adhesion is comparable with the dimension of MC3T3-pre-osteoblasts cells (~ 14 μm). Thus, the variation of surface roughness opens the way to control and tailor the fraction of adhered cells, depending on the demand of medical techniques.

## Introduction

Titanium and its alloys are widely employed in medicine. They are used in the manufacture of artificial heart valves, stents of blood vessels, endoprostheses of bones and joints (shoulder, knee, hip, elbow), for reconstruction of the auricles, in facial surgery, and also as dental and ophthalmological implants [1–7]. The use of titanium alloys in medicine falls into two broad classes. First, these are long-term implants. They, if possible, should exist indefinitely long in the patient's body without replacement. The second class of titanium products is used for temporary fixation of bone fragments until the bones grow together. Then these metal structures are removed, and,

conversely, they should not grow together with the bone. The process of forming a contact between the cells of a living organism and a titanium implant is very complex and includes many different stages. The first phase of cell/material interaction includes attachment, adhesion, and spreading of cells. The quality of this first phase determines the cell's capacity to proliferate and to differentiate itself on contact with the implant. It has been demonstrated that cell adhesion and/or differentiation of osteoblasts depends on the nano- and microtopography of the metallic surface [8–10]. For production of nanorelief on the Ti alloys, the processes like dealloying, anodization, and plasma sputtering were employed [11, 12]. The nanoroughening of the

surface influences the adhesion, proliferation, and differentiation of cells *in vitro*, as well as osseointegration *in vivo* [13, 14]. For successful development of new Ti alloys for medical applications, the effect of surface roughness and/or morphology on the process of interaction of the cells of a living organism with the implant should be clearly separated from the effects of other factors, such as chemical and phase composition of the alloy, or the grain size and grain texture. This is because the surface morphology can conceal or disturb the influence of other factors. Therefore, a controllable method for creating the desired roughness and/or surface morphology is needed. We note in this context that preparing the implant surface by mechanical grinding and polishing, on the one hand, is very simple. It is often considered as just one of the preparatory steps for other methods of surface treatment. On the other hand, it is very effective in generating both random roughness and controlled surface profiles with directional grooves. There is a lot of evidence in the literature in favor of this approach [1–5, 15]. Therefore, the aim of this work was to investigate the effect of surface roughness of the standard titanium alloy Ti-6Al-4V (which will be used as a control in future studies) on the adhesion of human cells. The rough surfaces with directional grooves were fabricated by mechanical grinding with a wide range of abrasive materials with a systematically changing size of abrasive grains.

Various methods of chemical and physical treatment of titanium, such as polishing, sandblasting, plasma spraying, acid etching, or bioactive coatings, have been used to improve cell adhesion, resulting in faster bone integration *in vivo* [16, 17]. In turn, the process of forming a contact between bone and a Ti implant is influenced by many different factors. One of the very important factors is the roughness (or smoothness) of the implant surface. The effect of surface roughness on the process of bone fusion of a living organism and an implant was discovered back in the 1970s. Since then, many studies have been devoted to the influence of surface roughness. A variety of techniques have been developed to control surface morphology of titanium implants. Among them are powder sintering [18, 19], mechanical machining [20, 21], mechanical grinding and polishing [7, 22, 23], blasting [6, 20–30], chemical etching [3, 20, 22, 30–38], etching of inkjet printed patterns [39–41], electrochemical anodization [22], selective infiltration etching [18, 42, 43], laser ablation [29, 44–50], selective laser melting and surface texturing [18, 51], laser shock peening [52–54], electric discharge machining [3, 55–60], microdrilling [61], ultrasonic-assisted machining [62–69], electrochemical machining [70–72], electrochemical anodization and hydrothermal processing [22, 73, 74], and electron beam patterning [75, 76]. These methods enable producing both the surfaces with random roughness (which is well-characterized by the  $R_a$  parameter being the mean root square deviation of the surface height from the average level), as well as the surfaces with periodic patterns,

such as ordered systems of holes and protrusions, or various grooves [15].

The goal of this work was to study the cell adhesion to the Ti-6Al-4V substrates with controlled roughness. This controlled roughness was the array of linear grooves with different width and depth produced by the abrasive media with different sizes of the abrasive grains. The linear grooves on the Ti-6Al-4V substrates were manufactured with a set of abrasive SiC papers with grit sizes of 220, 400, 600, 600, 1000, 1200, 2000, and 4000 (number of grains per  $\text{cm}^2$ ) (these grit sizes correspond to the SiC grain size of 68–7  $\mu\text{m}$ ) and polished with diamond pastes with grain sizes of 6, 3, and 1  $\mu\text{m}$ . Thus, the surfaces with the parallel grooves of ten different characteristic dimensions (width and depth) from 1 to 68  $\mu\text{m}$  were studied. The mean size of the MC3T3-pre-osteoblasts cells is about ~14  $\mu\text{m}$  and is, therefore, within the studied interval of grooves' dimensions.

## Results

The disks of cold-wrought Ti-6 wt%Al-4 wt%V alloy (also known as VT6) were sequentially ground with abrasive SiC papers with grit sizes of 220, 400, 600, 600, 1000, 1200, 2000, and 4000 (number of grains per  $\text{cm}^2$ ) and polished with diamond pastes with grain sizes of 6, 3, and 1  $\mu\text{m}$ . The grinding (and/or polishing) process has been interrupted at a certain grain size in order to obtain different surface roughness. Moreover, at the last stage, the samples were ground (or polished) by hand unidirectionally in order to obtain the array of (more or less) parallel grooves on the surface. Such grooves have different width and depth, depending on the grain size of abrasive SiC papers or diamond pastes. In Fig. 1, the light micrographs are shown for the Ti-6Al-4V (VT6) alloy samples ground with various SiC papers and polished with diamond paste. The nominal grain size of diamond suspension is (a) 6  $\mu\text{m}$ , and of grinding paper is (b) 10  $\mu\text{m}$  (2000 grit), (c) 15  $\mu\text{m}$  (1200 grit), (d) 18  $\mu\text{m}$  (1000 grit), (e) 22  $\mu\text{m}$  (800 grit), (f) 35  $\mu\text{m}$  (400 grit), and (g) 68  $\mu\text{m}$  (220 grit).

It is clearly visible in all the micrographs that the unidirectional grinding during the last step allowed indeed to produce the array of almost parallel scratches on the surface of Ti-6Al-4V (VT6) alloy. The scratches become finer with increasing grit number of abrasive paper (i.e., decreasing abrasive grain size). As expected, the finest and the smoothest are the samples after polishing with diamond paste [Fig. 1(a)].

In Fig. 2, the 3D-micrographs obtained using the confocal light microscopy are shown for the same sample set as in Fig. 1. Again, they are both for samples only ground with the abrasive paper [Fig. 2(b)–(g)] as well as for samples polished with diamond paste [Fig. 2(a)]. It can be clearly seen that all these samples contain the set of unidirectional grooves. These grooves

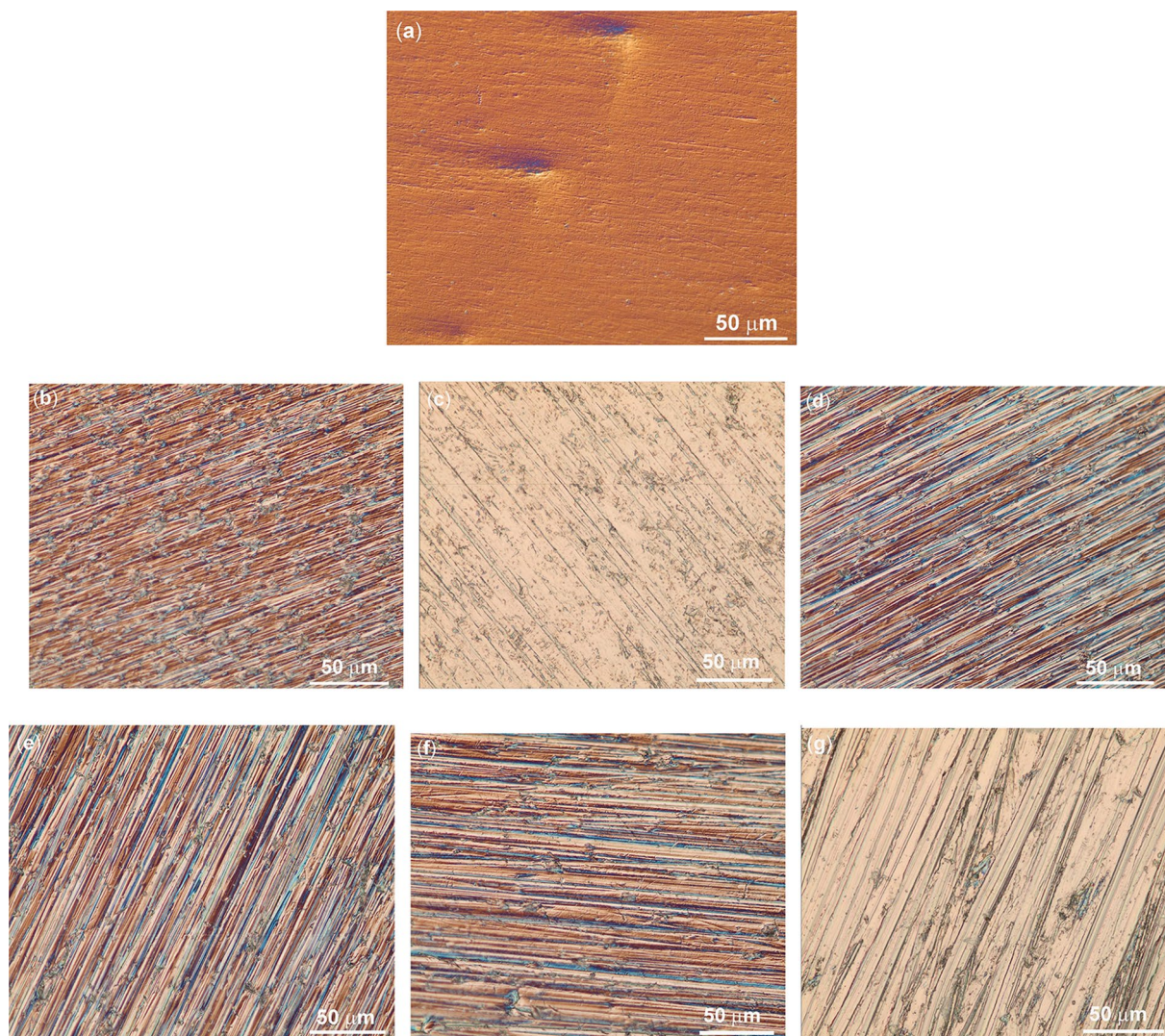


**Figure 1:** Light micrographs for the Ti-6Al-4V (VT6) alloy samples ground with various SiC papers and polished with diamond paste. The nominal grain size of diamond suspension is (a) 6  $\mu\text{m}$  and of grinding paper is (b) 10  $\mu\text{m}$  (2000 grit), (c) 15  $\mu\text{m}$  (1200 grit), (d) 18  $\mu\text{m}$  (1000 grit), (e) 22  $\mu\text{m}$  (800 grit), (f) 35  $\mu\text{m}$  (400 grit), and (g) 68  $\mu\text{m}$  (220 grit).

become narrower and shallower with decreasing grain size of the grinding paper or of the polishing suspension.

The confocal light microscopy allowed quantifying the parameters of surface roughness obtained by the unidirectional grinding and polishing of Ti-6Al-4V (VT6) alloy samples. Figure 3 shows the examples of height profiles obtained with the aid of confocal light microscopy for three samples, namely for two samples ground with the abrasive paper with grit size of (a) 220 grit (abrasive grain size 68  $\mu\text{m}$ ) and (b) 1200 (abrasive grain size 15  $\mu\text{m}$ ), and (c) for the sample polished with diamond paste 1  $\mu\text{m}$ . It is clearly visible how the surface roughness becomes finer with increasing grit number of abrasive paper (i.e., decreasing abrasive grain size) and transition from grinding paper to the polishing suspension. The topography is ordered or even has quasiperiodic character.

Such curves enabled quantifying the roughness-height parameters for all studied samples using the ISO 25178 standard (see Tables 1 and 2).

Thus, we can see from the Tables 1, 2, and 3 as well as from the micrographs in Figs. 1 and 2 that the proposed grinding methods allowed us to manufacture the set of eleven substrates with a pattern of parallel quasiperiodic grooves. These grooves “start” from rather rough set with roughness amplitude of  $S_q = 1.01 \mu\text{m}$  and the maximum peak height of  $S_p = 6.13 \mu\text{m}$ , and interpeak distance of  $D_p = 6.1 \mu\text{m}$  for the grinding paper of 220 grit (grain size 68  $\mu\text{m}$ ). The grooves become continuously shallower and narrower in the set, with the smoothest sample polished using diamond paste with grain size of 1  $\mu\text{m}$  exhibiting the following roughness parameters:  $S_q = 0.087 \mu\text{m}$ ,  $S_p = 0.15 \mu\text{m}$ .

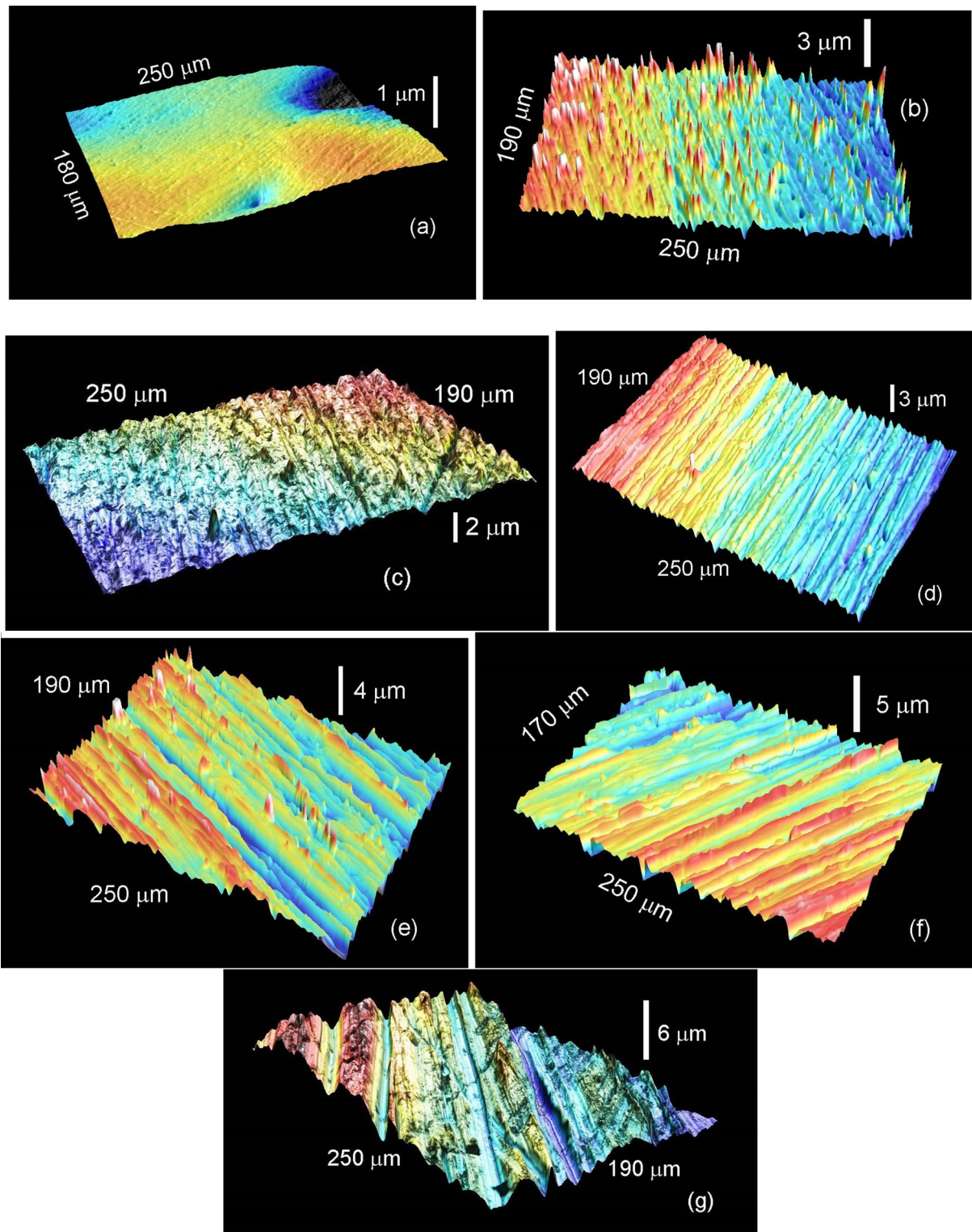


**Figure 2:** The micrographs obtained using the confocal light microscopy for the Ti-6Al-4V (VT6) alloy samples ground with various SiC papers and polished with diamond paste. The nominal grain size of diamond suspension is (a) 6  $\mu\text{m}$  and of grinding paper is (b) 10  $\mu\text{m}$  (2000 grit), (c) 15  $\mu\text{m}$  (1200 grit), (d) 18  $\mu\text{m}$  (1000 grit), (e) 22  $\mu\text{m}$  (800 grit), (f) 35  $\mu\text{m}$  (400 grit), and (g) 68  $\mu\text{m}$  (220 grit).

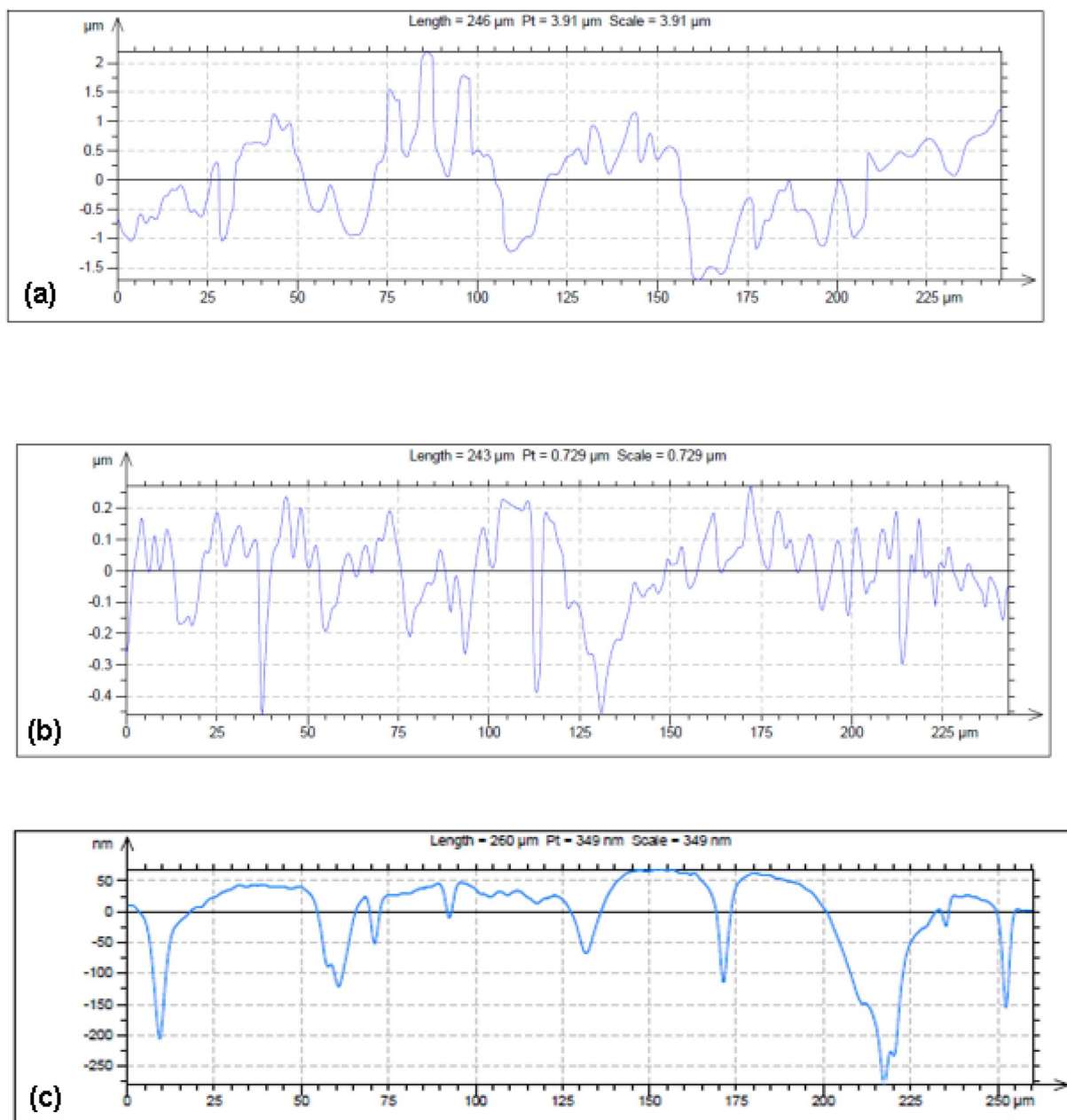


**Figure 3:** The height profiles obtained with the aid of confocal light microscopy for the sample ground with the abrasive paper (a) 220 grit (abrasive grain size 68 μm), (b) 1200 grit (abrasive grain size 15 μm), and (c) diamond paste 1 μm.

This set of substrates was used for the cell culture experiments with mouse MC3T3-pre-osteoblasts cells. In order to evaluate the effects of Ti-6Al-4V surface treatments on cells, initially all the metal samples were subjected to ultrasonic cleaning and series of consecutive washes with 60% ethanol and sterile distilled deionized ultrapure water. Alloy samples were placed per well of 24-well plate and cells were carefully seeded on the surface of the samples. The growth medium incubated at the same volume and conditions was used as control. After incubation for 30 min, the samples were washed by

DPBS, treated by Calcium AM, and observed with fluorescent microscope.

Figure 4 shows the obtained fluorescent micrographs of the MC3T3 cells treated by Calcein AM, which appears green, for the same set of samples as in Figs. 1 and 2. The micrographs illustrate the dependence of cell adhesion on the Ti-6Al-4V (VT6) alloy substrates with different surface roughness.

Figure 5 demonstrates the influence of the surface microrelief of the Ti-6Al-4V (VT6) alloy on the MC3T3 cell adhesion (i.e., relative fraction of adhered cells in comparison with control

**TABLE 1:** Roughness parameters (standard ISO 25178 and additional) of the Ti-6Al-4V (VT6) alloy samples after abrasive paper grinding.

Abrasive paper	Grain size, $\mu\text{m}$	Roughness amplitude parameters ISO 25178					Interpeak distance $D_{pr}$ $\mu\text{m}$
		$S_{qr}$ $\mu\text{m}$	$S_{pr}$ $\mu\text{m}$	$S_{vr}$ $\mu\text{m}$	$S_{zv}$ $\mu\text{m}$	$S_{ar}$ $\mu\text{m}$	
P220	68	1.011	6.13	4.68	10.82	0.804	$6.1 \pm 0.6$
P400	35	0.38	2.04	6.975	9.02	0.260	$4.8 \pm 0.1$
P600	27	0.21	1.24	1.53	2.775	0.160	$4.8 \pm 0.2$
P800	22	0.28	1.435	4.32	5.74	0.188	$5.0 \pm 0.5$
P1000	18	0.14	0.32	0.95	2.27	0.104	$4.6 \pm 0.3$
P1200	15	0.16	1.30	1.32	2.62	0.115	$4.6 \pm 0.2$
P2000	10	0.11	0.935	0.725	1.66	0.079	$4.7 \pm 0.3$
P4000	7	0.062	0.33	0.530	0.86	0.047	$3.9 \pm 0.1$

**TABLE 2:** Roughness parameters ISO 25178 of the Ti-6Al-4V (VT6) alloy samples after diamond paste polishing.

Diamond paste grain size, $\mu\text{m}$	Roughness amplitude parameters ISO 25178				
	$S_{qr}$ $\mu\text{m}$	$S_{pr}$ $\mu\text{m}$	$S_{vr}$ $\mu\text{m}$	$S_{zv}$ $\mu\text{m}$	$S_{ar}$ $\mu\text{m}$
6	0.15	0.32	0.87	1.19	0.107
3	0.199	0.47	1.43	1.9	0.141
1	0.087	0.15	0.43	0.58	0.065

**TABLE 3:** Chemical composition (wt%) of the investigated samples.

Element	Al	V	Zr	Ti
GOST 19807-91	5.3–6.8	3.5–5.3	< 0.3	Balance
Actual VT6 samples	$5.97 \pm 0.37$	$3.87 \pm 0.37$	Not detected	Balance

being 1). The data obtained showed that modification of the surface roughness of the Ti-6Al-4V (VT6) alloy samples significantly influenced the cell adhesion. The fraction of adhered cells behaves non-monotonously with the abrasive grain size. It is about 0.35 for grain size of 1  $\mu\text{m}$ , increases with increasing grain size up to 0.95 for grain size of 7  $\mu\text{m}$  and then slowly decreases down to 0.55 for abrasive grain size of 68  $\mu\text{m}$ .

We can suppose that the surface roughness parameters of Ti-6Al-4V (VT6) alloy (1–10  $\mu\text{m}$ ) correlate with the depth and width of scratches produced on the initially flat surface of the alloy. Therefore, it turns out that the microrelief of scratches produced by the grinding media with a grain size of about 10  $\mu\text{m}$  promoted cell adhesion to the greatest extent. In general, when studying the roughness interval of 1–10  $\mu\text{m}$ , we observed an increase in cell adhesion with an increase in the width and depth of scratches on the surface of alloy samples. The further coarsening of the relief contributed to a decrease of adhered cell count (Fig. 6). Thus, we observe the bell-shaped form of the dependence of the cell adhesion strength on the characteristics of the surface microrelief (width and depth of scratches), while the maximum values of adhesion are provided by the microrelief

produced by a grinding media with a grain size in the range of 10–20  $\mu\text{m}$ .

Figure 6 shows the results of the analysis of the cell size [Fig. 6(a)] and clustering [Fig. 6(b)] of the MC3T3 cells in a suspension. The results obtained on a cell analyzer demonstrate that the level of clustering of the cells was low, with 79% of the cells being single. Based on this, we can assert that the linear dimensions of the cells ranged from 4 to 40  $\mu\text{m}$ , with the mean and median cell size being 17.8 and 14.3  $\mu\text{m}$ , respectively [Fig. 6(a)]. These results suggest that the maximum level of cell adhesion can be achieved when the characteristic particle size of the grinding media is commensurate with the linear dimensions of most of the cells (from 10 to 18  $\mu\text{m}$ ). It is quite possible that when examining other cells with different dimensions, the roughness of the surface optimal for cell adhesion would be different.

## Discussion

As we already mentioned in the Introduction, many studies had been devoted to the influence of surface roughness on the properties of titanium implants. Many different methods were developed to control their surface morphology. We have to mention here the powder sintering [18, 19], mechanical machining [20, 21], mechanical grinding and polishing [7, 22, 23], blasting [6, 20–30], chemical etching [3, 20, 22, 30–38], etching of inkjet printed patterns [39–41], electrochemical anodization [22], selective infiltration etching [18, 42, 43], laser ablation [29, 44–50], selective laser melting and surface texturing [18, 51], laser shock peening [52–54], electric discharge machining [3, 55–60], microdrilling [61], ultrasonic-assisted machining [62–69], electrochemical machining [70–72], electrochemical anodization and hydrothermal processing [22, 73, 74], and electron beam patterning [75, 76]. In all these papers, the properties of titanium implants were compared usually for the restricted number of roughness values.

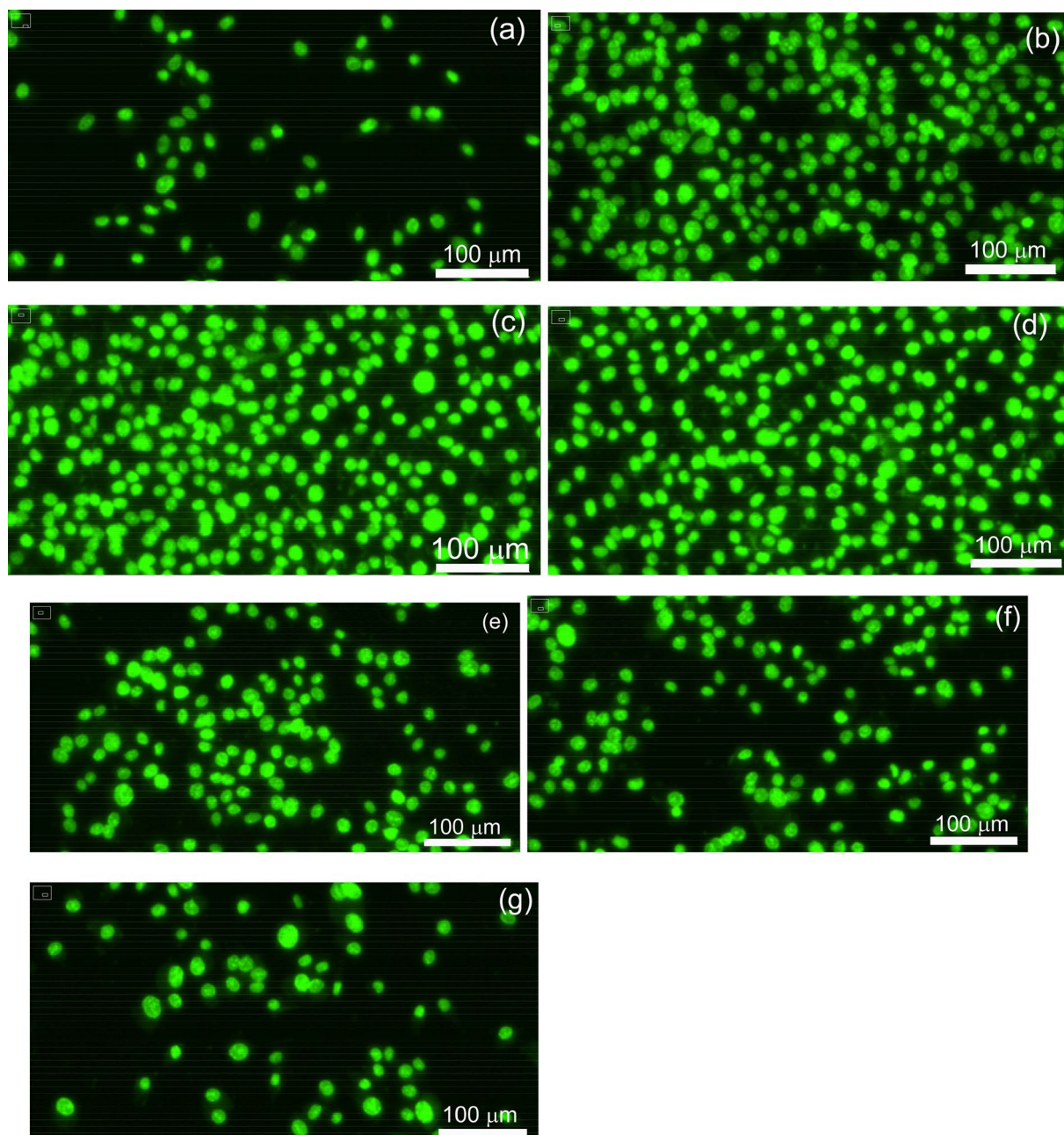


**Figure 4:** The micrographs obtained with fluorescent microscopy of the MC3T3 cells adhered on the Ti-6Al-4V (VT6) alloy. The cells were treated by Calcein AM and appeared green. The nominal grain size of diamond suspension is (a) 6  $\mu\text{m}$  and of grinding paper is (b) 10  $\mu\text{m}$  (2000 grit), (c) 15  $\mu\text{m}$  (1200 grit), (d) 18  $\mu\text{m}$  (1000 grit), (e) 22  $\mu\text{m}$  (800 grit), (f) 35  $\mu\text{m}$  (400 grit), and (g) 68  $\mu\text{m}$  (220 grit).

The goal of our work was to create the rather broad set of samples with continuously changing values of depth and width of linear (more or less parallel) grooves on the surface. This set of the substrates was tested for the adhesion of mouse MC3T3-pre-osteoblasts cells after 30 min of contact. Surprisingly, the fraction of adhered MC3T3 cells exhibits a non-monotonous dependence on the surface roughness. The fraction of adhered cells is about 0.35 for polishing media

grain size of 1  $\mu\text{m}$ , then it increases with increasing grain size up to 0.95 for grain size of 7  $\mu\text{m}$ , and afterward slowly decreases down to 0.55 for abrasive grain size of 68  $\mu\text{m}$ . Thus, the substrate with grooves with abrasive grain size of about 10  $\mu\text{m}$  promoted cell adhesion to the greatest extent. In turn, the grain size corresponding to the maximum cells adhesion is comparable with the dimension of MC3T3-pre-osteoblasts cells ( $\sim 14 \mu\text{m}$ ). This conclusion could be reached only due to

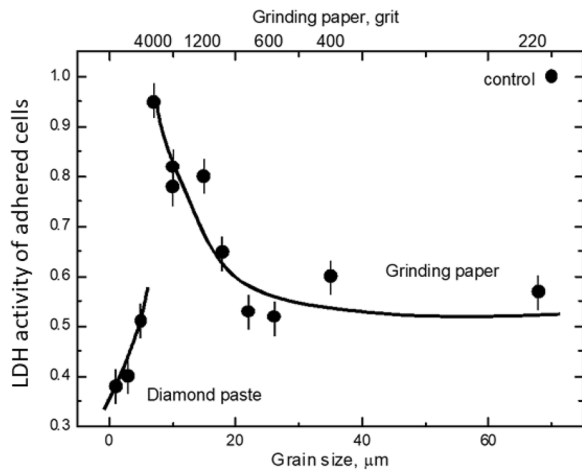


**Figure 5:** Influence of the surface microrelief of the Ti-6Al-4V (VT6) alloy on the fraction of adhered MC3T3 cells. The abscissa shows the nominal grain size of grinding paper (from 7  $\mu\text{m}$  and above) or diamond suspension (below 7  $\mu\text{m}$ ). The lines are the guides for the eye. Two lines show two kinds of the surface preparation: only grinding (right part of the figure) or polishing with diamond paste after grinding (left part).

the large number of the samples and broad set of roughness parameters.

It is interesting that while the correlation between cells adhesion and the grain size of the grinding/polishing media is quite obvious (see Fig. 5), the relationship between cells adhesion and average interpeak distance of surface topography profiles is less clear. Indeed, the interpeak distance is approximately constant (4.6–5.0  $\mu\text{m}$ ) for the wide range of grinding media grain sizes (10–35  $\mu\text{m}$ , see Table 1). A closer inspection of topography profiles in Fig. 3(a), (b) reveals a hierarchical nature of surface roughness, with numerous minor local peaks dotting the global quasiperiodic variations of surface profile, with the characteristic distance between the global minima/maxima approximately corresponding to the

grain size of the grinding media. Determining a characteristic distance between such global extrema in a statistically reliable way is a formidable mathematical problem that will be handled in our forthcoming works.

It is known that the complicated surface microrelief of the substrate can significantly modulate the cell cycle and reactivity of mesenchymal cells, stimulating adhesion [77]. In this regard, the use of various manipulations and processing methods that contribute to the development of the surface of the future submersible implant for osteosynthesis can have a significant impact on the outcome of its clinical use. Stimulation of adhesion of mesenchymal cells, including cells with osteogenic potential, mediates the acceleration of fixation and osseointegration of the implant, reducing the risk of postoperative complications of osteosynthesis in the form of migration of metal structures, the threat of soft tissue perforation, or the lack of supportability of the reconstructed bone, whereas an excessively smooth product surface may inhibit long-term cellular reactivity. In particular, Sinha et al. reported a decrease in cell membrane expression of  $\alpha 5$  integrin molecules mediating prolonged adhesion due to contact with a polished substrate [77, 78]. The use of implants with a smooth surface can be justified as a temporary construction to compensate for the anatomical configuration and mechanical strength of the restored bone or joint. In this case, the lack of osseointegration will greatly simplify the extraction of the implant, reducing the risk of trauma to the surrounding tissues. Also, the use of implants that suppress cellular reactivity is justified when they are used as intravascular stents or substitutes for articular surfaces, when the adhesion of leukocytes, platelets, or fibrin can deprive the medical device of its functionality.

Titanium and its alloy Ti-6Al-4V are widely used in medical implants such as artificial joint endoprostheses, fracture fixation devices, and dental implants due to their high hardness and excellent biocompatibility [79]. However, it is known

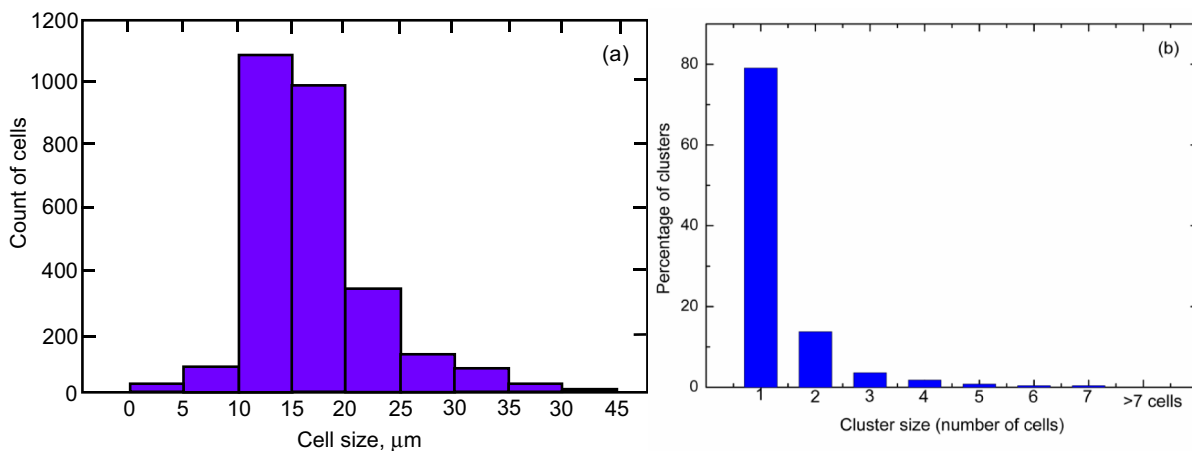


**Figure 6:** Analysis of the cell size (a) and clustering (b) of the MC3T3 cell suspension loaded on the Ti-6Al-4V (VT6) alloy substrate.

that titanium weakly stimulates adhesion and proliferation of stromal osteogenic cells, which inhibits its osseointegration and can lead to osteolysis followed by re-fracture [80]. This determines the importance of modifying the surface composition or microstructure of implantable medical devices with the aim of improving cell adhesion, which is intended to ensure the wider use of Ti and its alloys in orthopedics, especially as articular components for total joint replacement.

Many studies have demonstrated that nano- and micro-topography of a biomaterial can influence cell adhesion and/or differentiation of osteoblasts [8, 9]. Micro- or nano-roughness of metal surfaces plays an important role in the formation of physical interaction between osteoblasts and metal surfaces [10]. To create a nanorelief of titanium alloys, various approaches were used, such as dealloying, anodization, and plasma sputtering induced by target ions [11, 12]. The nanomodified surface of titanium alloys contributed to the improvement of cytocompatibility due to the interaction of cells with the formed titanium nanostructures. It has been shown that nanoroughening of the surface of titanium alloys promotes adhesion, proliferation, and differentiation of cells on cells in vitro and promotes osseointegration of implants in vivo [13]. Biocompatibility was confirmed by assessing the attachment, proliferation, and differentiation of osteoblast cells. The cell adhesion was improved in all nanostructured groups of zero charge point due to the formation of focal adhesions in which cells show strong interaction with nanostructured surfaces. Such surfaces can trigger biologically active cellular responses by controlling integrin-dependent cell adhesion signaling pathways. The results indicated that a specific morphological state (nanostructure width  $\geq 130$  nm) was required to achieve superior osteoblast cell adhesion as well as cell proliferation and differentiation [14]. Despite these advances, the complex and time-consuming process of dealloying and the low stability of the coating between the anodic oxidation layer and the titanium of the anodizing process remain serious limitations of these approaches [81]. No less important for cellular behavior is microtopography of the biomaterial. Thus, in the study of bioceramics, it was found that human mesenchymal stem cells grown in grooves no larger than  $135 \mu\text{m}$  showed a higher expression of alkaline phosphatase and collagen I [82], and hemispherical depressions  $440 \mu\text{m}$  in size promoted cell growth and gene and protein expression of osteocalcin [83]. On this basis, the authors concluded that macro-architectonics can promote osteogenesis and, in particular, osteoblast differentiation due to increased intercellular interactions [84]. An in vitro study of titanium alloy Ti6Al4V demonstrated that osteogenic differentiation of cells was higher when the surface had a texture with micron roughness [85].

Similar results were obtained using a Ti6Al4V alloy sandblasted to create micron-scale roughness [86]. The microroughness of the metal surface enhances the differentiation of

osteoblasts and contributes to the enhancement of osteogenesis and osseointegration in vivo. The conducted studies indicate that surface microtopography is an important factor determining the biological interactions between tissue and biomaterials. In vivo studies have shown that bone tends to form on surfaces with micrometer roughness, while fibrous connective tissue forms on smooth surfaces [87, 88]. Previous studies examining the effect of titanium microstructure on the response of MG63 cells found that a sulcus depth of  $3.0 \mu\text{m}$  is a factor in osteogenic differentiation [89, 90]. The microroughness of the titanium alloy surface modulated the ability of MG63 cells to synthesize and secrete autocrine and paracrine osteogenic bone mediators. As surface roughness increased, levels of prostaglandin E2, TGF- $\beta$ 1 and osteoprotegerin also increased. [91]. In the works of other researchers, it was found that the grooves of the substrate microrelief of about  $10 \mu\text{m}$  in size actively stimulated the survival and adhesion of osteogenic cells [48, 92, 93]. The results obtained in the present work indicate that a change in the microstructure of the surface of titanium alloys leads to the stimulation of cell adhesion, while samples treated with an abrasive with a grain size of  $10$  to  $18 \mu\text{m}$  stimulated cell adhesion most actively. At the same time, the processing of substrates with fine diamond paste ( $6 \mu\text{m}$ ) resulted in minimal cell adhesion. As follows from the presented data, not only the width of the grooves, but also their depth is optimal for stimulating the adhesion of osteogenic cells. At the same time, both too deep ( $S_z = 9.02$ – $10.82 \mu\text{m}$ ) and shallow grooves ( $S_z = 0.86 \mu\text{m}$ ) had the least effect on the functional state of the cells. Our studies allow us to conclude that the modification of the microtopography of the surface of titanium alloys should provide a microrelief formed by grooves about  $5 \mu\text{m}$  wide and about  $2 \mu\text{m}$  deep to ensure effective adhesion of osteogenic cells on the biomaterial. This approach can increase the efficiency of using bone bioimplants by accelerating the processes of osteogenic differentiation and osseointegration. These results confirm the assumptions made earlier about the need to take into account the surface structure when developing bioimplants based on a titanium alloy for the purposes of traumatology and orthopedics.

## Conclusions

We can conclude that the experimental results obtained in this study are promising for the development of implantable metal structures for osteosynthesis, which remains an extremely urgent problem for medical and veterinary clinical practice. Our results indicate that an ordered microrelief produced by mechanical treatment of the alloys surface can stimulate the surface adhesion of osteogenic cells. We identified the parameters of grinding/polishing media and the corresponding surface topography parameters resulting in enhanced cell adhesion. The processing method described in this work can be employed in

finishing of the implants for osteoreconstructive surgery. The implants made of the Ti-6Al-4V alloy are widely used in clinical practice due to their high strength-to-weight ratio, efficiency in replacing bone defects, as well as biocompatibility and corrosion resistance. We demonstrated that surface microrelief consisting of parallel grooves produced by grinding media with a grain size of 10–18 μm stimulates the adhesion of cells with osteogenic potential on the implant surface. This in turn will contribute to stable fixation of osteosynthesis and accelerated osseointegration of the metal structure after implantation.

## Materials and methods

For the investigations, the Ti-6 wt%Al-4 wt% V alloy of commercial purity has been used (VSMPO-AVISMA, Verkhnyaya Salda, Russia). The alloy is also known as VT6 according to Russian standard GOST 19807-91 [94]. The alloy was supplied as cold-wrought bar of 10 mm in diameter. The chemical composition of the samples was verified using scanning electron microscopy (SEM) and X-ray microanalysis on a Tescan Vega TS5130 MM instrument (Tescan Orsay Holding a.s., Brno, Czech Republic) equipped with an energy dispersive spectrometer INCA Energy 450 manufactured by Oxford Instruments Industrial Ltd., Abingdon, Oxon, UK (see Table 3).

The 2 mm thick disks have been mechanically cut from the bar. The obtained disks were sequentially ground with abrasive SiC papers with grit sizes of 220, 400, 600, 600, 1000, 1200, 2000, and 4000 (number of grains per cm<sup>2</sup>) and polished with diamond pastes with grain sizes of 6, 3, and 1 μm. According to the FEPA standard [95], the SiC papers with these grit sizes correspond to the SiC grain size of 68–7 μm, (see Table 4). The samples were ground using home-made grinding machine. This grinding process was performed under similar experimental conditions (grinding time 2 min, pressure 4 × 10<sup>4</sup> Pa) in each case. The grinding (and/or polishing) process has been interrupted at a certain grain size in order to obtain different surface roughness. Moreover, at the last stage, the samples were ground (or polished) by hand unidirectionally in order to obtain the array of (more or less) parallel grooves on the surface. Such grooves have different width and depth, depending on the grain size of abrasive SiC papers or diamond pastes (see micrographs in Figs. 1, 2).

Surface topography of the samples was examined by several techniques:

- (a) Light microscopy (Olympus BX51 microscope (Olympus corp., Tokyo, Japan)) using the “Stream Essentials” software (Olympus corp., Tokyo, Japan) provided general view at magnifications × 100 and × 500.
- (b) Detailed investigation of the topography (at × 20 and × 50 magnification) with quantitative evaluation of the roughness parameters was performed using the surface confocal light microscope Leica DCM3D (Leica Microsystems, Wezlar, Germany).
- (c) High-resolution SEM (Zeiss Ultra-Plus FEG-SEM, Carl Zeiss AG, Oberkochen, Germany).

The SensoMap Turbo 5.1.15450 software of the confocal microscope provided calculation of standard roughness parameters according to ISO 25178 standard (being mostly “amplitude parameters” from Biggerelle et al. classification [96], based on height distribution). Thus, we determined the  $S_q$ ,  $S_p$ ,  $S_v$ ,  $S_z$ , and  $S_a$  roughness parameters according ISO 25178.  $S_q$  is the root mean square height of the scale-limited surface (i.e., the root mean square value of the ordinate values within a definition area A):

$$S_q = \sqrt{\frac{1}{A} \int \int_A Z^2(x, y) dx dy} \quad (1)$$

$S_p$  is the maximum peak height of the scale-limited surface (i.e., largest peak height value within a definition area).  $S_v$  is the maximum pit height of the scale-limited surface (i.e., minus the smallest pit height value within a definition area).  $S_z$  is the maximum height of the scale-limited surface (i.e., sum of the maximum peak height value and the maximum pit height value within a definition area).  $S_a$  is the arithmetical mean height of the scale-limited surface (i.e., arithmetic mean of the absolute of the ordinate values within a definition area A):

$$S_a = \frac{1}{A} \int \int_A |Z(x, y)| dx dy \quad (2)$$

Several works dealing with quantitative roughness description [96–98] considered that using these parameters only might be sometimes insufficient, and they recommended to add a spatial feature parameter based on peak counting. For example, Biggerelle et al. [98], used the  $N_p$  parameter of being the number of peaks per inch.

By analogy, our investigation included also an additional quantitative “width” value, namely a distance between peaks,  $D_p$ ,

**TABLE 4:** Abrasive materials used for the investigation.

Abrasive paper (according to FEPA <sup>a</sup> grades)	P220	P400	P600	P800	P1000	P1200	P2000	P4000
Average abrasive grain size, μm [104]	68	35	27	22	18	15	10	7

<sup>a</sup>FEPA is Federation of European Producers of Abrasives.

that seemed to be relevant to biocompatibility of the investigated samples. The value of these additional parameters was calculated from profile lines (being orthogonal to grinding direction) of the surfaces scanned by the confocal microscope at  $\times 50$  magnification. The distance between peaks was determined as  $D_p = L/N_p$ , where  $L$  is the length of a profile line ( $\mu\text{m}$ ) and  $N_p$  is the number of peaks within the line.

Mouse MC3T3-pre-osteoblasts cells (the collection of N.N.Blokhin NMRC of Oncology) were used in cell culture experiments. The cells were cultivated in humid atmosphere at  $37^\circ\text{C}$  with 5%  $\text{CO}_2$  in the growth medium based on Dulbecco's modified Eagle medium (DMEM) supplemented with 10% fetal bovine serum (FBS), 100 U/mL penicillin, 100  $\mu\text{g}/\text{ml}$  streptomycin, 2 mM L-glutamine (PanEco, Russia). In order to evaluate the effects of Ti-6Al-4V surface treatments on cells, initially all the metal samples were subjected to ultrasonic cleaning and series of consecutive washes with 60% ethanol and sterile distilled deionized ultrapure water.

Cells were treated with 0.05% trypsin, washed with Dubecco's Phosphate Buffer Saline (DPBS), and suspended in the growth medium ( $3.4 \times 10^6$  cells in 1 ml). Alloy samples were placed per well of 24-well plate (Corning, USA). 20  $\mu\text{l}$  of cells was carefully seeded on the surface of the samples. After incubation for 30 min, the samples were washed by DPBS, treated by Calcium AM (Invitrogen, Thermo Fisher Scientific, USA), and observed with Lionheart LX Automated Microscope (BioTek, USA). For quantitative analysis, we used the Lactate Dehydrogenase (LDH) Activity Assay Kit (Sigma-Aldrich, USA) after evaluating in triplets the optical density (OD) at 492 nm using plate reader Spark (Tecan, USA) in accordance with the manufacturer's recommendations. The growth medium incubated at the same volume and conditions was used as control. The LDH activity seeded on alloy sample evaluated as OD in wells with alloys/OD in control. The measurement results were presented as mean  $\pm$  standard deviation.

Quantification of lactate dehydrogenase (LDH) is a well-established routine assay for cell viability. We have investigated the relationship between cell concentration and total LDH activity in samples of cell lysate. Although there are differences in the amount of LDH present in different cell types, the total enzyme activity in a sample of cell lysate is directly proportional to the concentration of cells in the sample. The measurement of LDH activity in vitro provides a sensitive, accurate, and cost-effective alternative to the use of either radioisotopic or redox-based assays for the determination of cell numbers [99, 100]. In particular, this test is often used to evaluate of cell survival on the surface of alloys and other materials [101].

## Acknowledgments

The authors wish to thank Prof. Boaz Pokroy and Dr. Iryna Polishchuk for helpful discussions.

## Funding

This work was partially carried out within the framework of the state assignment of the Institute of Solid State Physics of the Russian Academy of Sciences, as well as with the financial assistance of the Russian Foundation for Basic Research (Grant 19-58-06002) and Israel Ministry of Science and Technology (Grant 3-16534).

## Data availability

Data are contained within the article.

## Declarations

**Conflict of interest** There is no conflict of interest or competing interests.

## References

1. K. Anselme, *Biomaterials* **21**, 667 (2000). [https://doi.org/10.1016/s0142-9612\(99\)00242-2](https://doi.org/10.1016/s0142-9612(99)00242-2)
2. K. Anselme, M. Bigerelle, B. Noel, E. Dufresne, D. Judas, A. Iost, P. Hardouin, *J. Biomed. Mater. Res.* **49**, 155 (2000). [https://doi.org/10.1002/\(SICI\)1097-4636\(200002\)49:2%3c155::AID-JBM2%3e3.0.CO;2-J](https://doi.org/10.1002/(SICI)1097-4636(200002)49:2%3c155::AID-JBM2%3e3.0.CO;2-J)
3. O. Zinger, K. Anselme, A. Denzer, P. Habersetzer, M. Wieland, J. Jeanfils, P. Hardouin, D. Landolt, *Biomaterials* **25**, 2695 (2004). <https://doi.org/10.1016/j.biomaterials.2003.09.111>
4. K. Anselme, M. Bigerelle, *Acta Biomater.* **1**, 211 (2005). <https://doi.org/10.1016/j.actbio.2015.11.007>
5. K. Anselme, M. Bigerelle, *Int. Mater. Rev.* **56**, 243 (2011). <https://doi.org/10.1179/1743280411Y.0000000001>
6. C. Zhou, F. Lei, J. Chodosh, E.I. Paschalis, *Ophthalmol. Vis. Sci.* **57**, 1927 (2016). <https://doi.org/10.1167/iovs.15-18406>
7. K. Anselme, P. Linez, M. Bigerelle, D. Le Maguer, A. Le Maguer, P. Hardouin, H.F. Hildebrand, A. Iost, J.M. Leroy, *Biomaterials* **21**, 1567 (2000). [https://doi.org/10.1016/s0142-9612\(00\)00042-9](https://doi.org/10.1016/s0142-9612(00)00042-9)
8. E. Saiz, E.A. Zimmermann, J.S. Lee, U.G.K. Wegst, A.P. Tomsia, *Dent. Mater.* **29**, 103 (2013). <https://doi.org/10.1016/j.dental.2012.08.001>
9. L. Xia, K. Lin, X. Jiang, B. Fang, Y. Xu, J. Liu, D. Zeng, M. Zhang, X. Zhang, J. Chang, Z. Zhang, *Biomaterials* **35**, 8514 (2014). <https://doi.org/10.1016/j.biomaterials.2014.06.028>
10. L. Damiani, M.G. Eales, A. Nobbs, B. Su, P.M. Tsimbouri, M. Salmeron-Sanchez, M. Dalby, *J. Tissue Eng.* **9**, 2041731418790694 (2018). <https://doi.org/10.1177/2041731418790694>
11. I.V. Okulov, S.-H. Joo, A. Okulov, A.S. Volegov, B. Luthringer, R. Willumeit-Römer, L. Zhang, L. Madler, J. Eckert, H. Kato, *Nanomaterials* **10**, 1479 (2020). <https://doi.org/10.3390/nano10081479>

12. J. Kim, H. Lee, T.-S. Jang, D. Kim, C.-B. Yoon, G. Han, H.-E. Kim, H.-D. Jung, *Metals* **11**, 618 (2021). <https://doi.org/10.3390/met11040618>
13. D.G. Bello, A. Fouillen, A. Badia, A. Nancy, *Acta Biomater.* **60**, 339 (2017). <https://doi.org/10.1016/j.actbio.2017.07.022>
14. J. Kim, H.N. Kim, K.-T. Lim, Y. Kim, S. Pandey, P. Garg, Y.-H. Choung, P.-H. Choung, K.-Y. Suh, J.H. Chung, *Biomaterials* **34**, 7257 (2013). <https://doi.org/10.1016/j.biomaterials.2013.06.029>
15. K. Anselme, M. Bigerelle, B. Noel, A. Iost, P. Hardouin, *J. Biomed. Mater. Res.* **60**, 529 (2002). <https://doi.org/10.1002/jbm.10101>
16. H. Wang, K. Su, L. Su, P. Liang, P. Ji, C. Wang, *J. Mech. Behav. Biomed. Mater.* **88**, 488 (2018). <https://doi.org/10.1016/j.jmbbm.2018.08.049>
17. B. Lohberger, N. Eck, D. Glaenger, H. Kaltenecker, A. Leithner, *Materials* **14**, 1574 (2021). <https://doi.org/10.3390/ma14061574>
18. D. Wang, G. He, Y. Tian, N. Ren, J. Ni, W. Liu, X. Zhang, *J. Mater. Sci. Technol.* **44**, 160 (2020)
19. R.A. Perez, G. Mestres, *Mater. Sci. Eng. C* **61**, 922 (2016). <https://doi.org/10.1016/j.msec.2015.12.087>
20. M. Lukaszewska-Kuska, P. Wirstlein, R. Majchrowski, B. Dorocka-Bobkowska, *Micron* **105**, 55 (2018). <https://doi.org/10.1016/j.msec.2015.12.087>
21. N.L. Khabilov, T.V. Melkumyan, T.O. Mun, F.K. Usmonov, I.M. Baybekov, *Int. J. Biomed.* **5**, 38 (2015)
22. M.M. Hatamleh, X. Wu, A. Alnazzawi, J. Watson, D. Watts, *Dent. Mater.* **34**, 676 (2018). <https://doi.org/10.1016/j.dental.2018.01.016>
23. V. Rutkunas, V. Bukelskiene, V. Sabaliauskas, E. Balciunas, M. Malinauskas, D. Baltriukiene, *J. Mater. Sci.: Mater. Med.* **26**, 169 (2015). <https://doi.org/10.1007/s10856-015-5481-8>
24. M. Kern, V. Thompson, *J. Dent.* **22**, 300 (1994). [https://doi.org/10.1016/0300-5712\(94\)90067-1](https://doi.org/10.1016/0300-5712(94)90067-1)
25. A. Wennerberg, *Int. J. Mach. Tools. Manuf.* **38**, 657 (1998). [https://doi.org/10.1016/S0890-6955\(97\)00114-4](https://doi.org/10.1016/S0890-6955(97)00114-4)
26. G.B. Valverde, R. Jimbo, H.S. Teixeira, E.A. Bonfante, M.N. Janal, P.G. Coelho, *Clin. Oral. Impl. Res.* **24**, 238 (2013). <https://doi.org/10.1111/j.1600-0501.2011.02392.x>
27. Z. Mohammadi, A. Ziaei-Moayyed, A.S.M. Mesgar, *J. Mater. Process. Technol.* **194**, 15 (2007). <https://doi.org/10.1016/j.jmatprotec.2007.03.119>
28. B. Arifvianto, K. Suyitno, M. Mahardika, *Surf. Coat. Technol.* **210**, 176 (2012). <https://doi.org/10.1016/j.surfcoat.2012.09.014>
29. A.B.H. Yoruç, E. Keleşoğlu, H.E. Yıldız, *Laser Med. Sci.* **34**, 1567 (2019). <https://doi.org/10.1007/s10103-019-02746-z>
30. A.E. Medvedev, A. Neumann, H.P. Ng, R. Lapovok, C. Kasper, T.C. Lowe, V.N. Anumalasetty, Y. Estrin, *Mater. Sci. Eng. C* **71**, 483 (2017). <https://doi.org/10.1016/j.msec.2016.10.035>
31. S. Bauer, P. Schmuki, K. von der Mark, Y. Park, *Prog. Mater. Sci.* **58**, 261 (2013). <https://doi.org/10.1016/j.pmatsci.2012.09.001>
32. D. Buser, T. Nydegger, T. Oxland, D.L. Cochran, R.K. Schenk, H.P. Hirt, D. Snétivy, L.P. Nolte, *J. Biomed. Mater. Res. Part A* **45**, 75 (1999). [https://doi.org/10.1002/\(SICI\)1097-4636\(199905\)45:2%3c75::AID-JBM1%3e3.0.CO;2-P](https://doi.org/10.1002/(SICI)1097-4636(199905)45:2%3c75::AID-JBM1%3e3.0.CO;2-P)
33. L.F. Cooper, Y. Zhou, J. Takebe, J. Guo, A. Abron, A. Holmén, J.E. Ellingsen, *Biomaterials* **27**, 926 (2006). <https://doi.org/10.1016/j.biomaterials.2005.07.009>
34. J.E. Ellingsen, C.B. Johansson, A. Wennerberg, A. Holmén, *Int. J. Oral Maxillofac. Impl.* **19**, 659 (2004). <https://doi.org/10.11607/jomi.2004.4.e>
35. D. Perrin, S. Szmukler-Moncler, C. Echikou, P. Pointaire, J.P. Bernard, *Clin. Oral Impl. Res.* **13**, 465 (2002). <https://doi.org/10.1034/j.1600-0501.2002.130504.x>
36. O. Zinger, G. Zhao, Z. Schwartz, J. Simpson, M. Wieland, D. Landolt, B. Boyan, *Biomaterials* **26**, 1837 (2005). <https://doi.org/10.1016/j.biomaterials.2004.06.035>
37. L. Pazos, P. Corengia, H. Svoboda, *J. Mech. Behav. Biomed. Mater.* **3**, 416 (2010). <https://doi.org/10.1016/j.jmbbm.2010.03.006>
38. T.F. Kuo, H.C. Lu, C.F. Tseng, J.C. Yang, S.F. Wang, T.C.K. Yang, S.Y. Lee, *J. Med. Biol. Eng.* **37**, 313 (2017). <https://doi.org/10.1007/s40846-017-0230-8>
39. A. Bruzzone, H. Costa, P. Lonardo, D.A. Lucca, *CIRP Ann. Manuf. Technol.* **57**, 750 (2008). <https://doi.org/10.1016/j.cirp.2008.09.003>
40. S.M. Basha, M. Bhuyan, M.M. Basha, N. Venkaiah, M.R. Sankar, *Mater. Today: Proc.* **26**, 2047 (2020). <https://doi.org/10.1016/j.matpr.2020.02.443>
41. I. Lauria, M. Kramer, T. Schröder, S. Kant, A. Hausmann, F. Böke, R. Leube, R. Telle, H. Fischer, *Acta Biomater.* **44**, 85 (2016). <https://doi.org/10.1016/j.actbio.2016.08.004>
42. M.N. Aboushelib, A.J. Feilzer, C.J. Kleverlaan, *J. Prosthodont.* **19**, 340 (2010). <https://doi.org/10.1111/j.1532-849X.2010.00575.x>
43. M.N. Aboushelib, N.A. Salem, A.L.A. Taleb, N.M.A. El Moniem, *J. Oral. Implantol.* **39**, 583 (2013). <https://doi.org/10.1563/AAID-JOI-D-11-00075>
44. A. Fasasi, S. Mwenifumbo, N. Rahbar, J. Chen, M. Li, A.C. Beye, C.B. Arnold, W.O. Soboyejo, *Mater. Sci. Eng. C* **29**, 5 (2009). <https://doi.org/10.1016/j.msec.2008.05.002>
45. W. Soboyejo, B. Nemetski, S. Allameh, C. Marcantonio, M.J. Ricci, *J. Biomed. Mater. Res. Part A* **62**, 56 (2002). <https://doi.org/10.1002/jbm.10221>
46. J. Chen, J. Ulerich, E. Abelev, A. Fasasi, C.B. Arnold, W.O. Soboyejo, *Mater. Sci. Eng. C* **29**, 1442 (2009). <https://doi.org/10.1016/j.msec.2008.11.014>
47. J. Chen, R. Bly, M. Saad, M.A. Al Khodary, R.M. El Backly, D.J. Cohen, N. Kattamis, M.M. Fatta, W.A. Moore, C.B. Arnold,

- M.K. Marei, W.O. Soboyejo, *Mater. Sci. Eng. C* **31**, 826 (2011). <https://doi.org/10.1016/j.msec.2010.12.019>
48. J. Chen, S. Mwenifumbo, C. Langhammer, J.P. McGovern, M. Li, A. Beye, W.O. Soboyejo, J. Biomed. Mater. Res. B Appl. Biomater. **82**, 360 (2007). <https://doi.org/10.1002/jbm.b.30741>
49. H.T. Lee, C.C. Lin, *Mater. Trans.* **60**, 1799 (2019). <https://doi.org/10.2320/matertrans.ME201909>
50. C. Zwahr, B. Voisiat, A. Welle, D. Günther, A.F. Lasagni, *Adv. Eng. Mater.* **20**, 1800160 (2018). <https://doi.org/10.1002/adem.201800160>
51. R. Kumaria, T. Scharnweber, W. Pflöging, H. Besser, J. Dutta Majumdar, *Appl. Surf. Sci.* **357**, 750 (2015). <https://doi.org/10.1016/j.apsusc.2015.08.255>
52. Y. Guo, R. Caslaru, *J. Mater. Process. Technol.* **211**, 729 (2011). <https://doi.org/10.1016/j.jmatprotec.2010.12.007>
53. C.S. Montross, T. Wei, L. Ye, G. Clark, Y.W. Mai, *Int. J. Fatigue* **24**, 1021 (2002). [https://doi.org/10.1016/S0142-1123\(02\)00022-1](https://doi.org/10.1016/S0142-1123(02)00022-1)
54. J.J. Ruschau, R. John, S.R. Thompson, T. Nicholas, *Int. J. Fatigue* **21**, S199 (1999). [https://doi.org/10.1016/S0142-1123\(99\)00072-9](https://doi.org/10.1016/S0142-1123(99)00072-9)
55. K. Ho, S. Newman, *Int. J. Mach. Tools Manuf.* **43**, 1287 (2003). [https://doi.org/10.1016/S0890-6955\(03\)00162-7](https://doi.org/10.1016/S0890-6955(03)00162-7)
56. C. Prakash, H.K. Kansal, B. Pabla, S. Puri, A. Aggarwal, *Proc. Inst. Mech. Eng.* **230**, 331 (2016). <https://doi.org/10.1177/0954405415579113>
57. P.W. Peng, K.L. Ou, H.C. Lin, Y.N. Pan, C.-H. Wang, *J. Alloys Compd.* **492**, 625 (2010). <https://doi.org/10.1016/j.jallcom.2009.11.197>
58. W.F. Lee, T.S. Yang, Y.C. Wu, P.W. Peng, *J. Exp. Clin. Med.* **5**, 92 (2013). <https://doi.org/10.1016/j.jecm.2013.04.002>
59. B.E.J. Lee, S. Ho, G. Mestres, M. Karlsson Ott, P. Koshy, K. Grandfield, *Surf. Coat. Technol.* **296**, 149 (2016). <https://doi.org/10.1016/j.surfcoat.2016.04.024>
60. M. Bigerelle, K. Anselme, B. Noel, I. Ruderman, P. Hardouin, A. Iost, *Biomaterials* **23**, 1563 (2002). [https://doi.org/10.1016/S0142-9612\(01\)00271-x](https://doi.org/10.1016/S0142-9612(01)00271-x)
61. T. Roy, D. Choudhury, S. Ghosh, A.B. Mamat, B. Pingguan-Murphy, *Ceram. Int.* **41**, 681 (2015). <https://doi.org/10.1016/j.ceramint.2014.08.123>
62. D. Brehl, T. Dow, *Precision Eng.* **32**, 153 (2008). <https://doi.org/10.1016/j.precisioneng.2007.08.003>
63. T. Thoe, D. Aspinwall, M. Wise, *Int. J. Mach. Tools. Manuf.* **38**, 239 (1998). [https://doi.org/10.1016/S0890-6955\(97\)00036-9](https://doi.org/10.1016/S0890-6955(97)00036-9)
64. G. Spur, S.E. Holl, *J. Mater. Process. Technol.* **62**, 287 (1996). [https://doi.org/10.1016/S0924-0136\(96\)02422-3](https://doi.org/10.1016/S0924-0136(96)02422-3)
65. Y.S. Dambatta, A.A. Sarhan, M. Sayuti, M. Hamdi, *Int. J. Adv. Manuf. Technol.* **92**, 3825 (2017). <https://doi.org/10.1007/s00170-017-0316-z>
66. T. Moriwaki, E. Shamoto, *CIRP Ann. Manuf. Technol.* **40**, 559 (1991). [https://doi.org/10.1016/S0007-8506\(07\)62053-8](https://doi.org/10.1016/S0007-8506(07)62053-8)
67. J. Gan, X. Wang, M. Zhou, B. Ngoi, Z. Zhong, *Int. J. Adv. Manuf. Technol.* **21**, 952 (2003). <https://doi.org/10.1007/s00170-002-1416-x>
68. J.D. Kim, I.H. Choi, *J. Mater. Process. Technol.* **68**, 89 (1997). [https://doi.org/10.1016/S0924-0136\(96\)02546-0](https://doi.org/10.1016/S0924-0136(96)02546-0)
69. S. Xu, T. Kuriyagawa, K. Shimada, M. Mizutani, *Front. Mech. Eng.* **12**, 33 (2017). <https://doi.org/10.1007/s11465-017-0422-5>
70. X. Lu, Y. Leng, *J. Mater. Process. Technol.* **169**, 173 (2005). <https://doi.org/10.1016/j.jmatprotec.2005.04.040>
71. C. Madore, O. Piotrowski, D. Landolt, *J. Electrochem. Soc.* **146**, 2526 (1999). <https://doi.org/10.1149/1.1391966>
72. T. Sjöström, B. Su, *Mater. Lett.* **65**, 3489 (2011). <https://doi.org/10.1016/j.matlet.2011.07.103>
73. H.T. Sirin, I. Vargel, T. Kutsal, P. Korkusuz, E. Piskin, *Artif. Cells Nanomed. Biotechnol.* **44**, 1023 (2016). <https://doi.org/10.3109/21691401.2015.1008512>
74. M. Zulfdesmi, A. Waki, K. Kuroda, M. Okido, *Mater. Sci. Eng. C* **42**, 405 (2014). <https://doi.org/10.1016/j.msec.2014.05.049>
75. C. Ramskogler, F. Warchomicka, S. Mostofi, A. Weinberg, C. Sommitsch, *Mater. Sci. Eng. C* **78**, 105 (2017). <https://doi.org/10.1016/j.msec.2017.03.311>
76. S. Gach, S. Olschok, U. Reisingen, *Materialwiss. Werkstofftech.* **50**, 365 (2019). <https://doi.org/10.1002/mawe.201981011>
77. K. Anselme, A. Ponche, M. Bigerelle, *Proc. Inst. Mech. Eng.* **224**, 1487 (2010). <https://doi.org/10.1243/09544119JEIM901>
78. R.K. Sinha, R.S. Tuan, *Bone* **18**, 451 (1996). [https://doi.org/10.1016/8756-3282\(96\)00044-0](https://doi.org/10.1016/8756-3282(96)00044-0)
79. A.N. Aufa, M.Z. Hassan, Z. Ismail, *J. Alloys Compd.* **896**, 163072 (2022). <https://doi.org/10.1016/j.jallcom.2021.163072>
80. D.A. Puleo, A. Nanci, *Biomaterials* **20**, 2311 (1999). [https://doi.org/10.1016/S0142-9612\(99\)00160-X](https://doi.org/10.1016/S0142-9612(99)00160-X)
81. M.-K. Lee, H. Lee, H.-E. Kim, E.-J. Lee, T.-S. Jang, H.-D. Jung, *Nanomaterials* **11**, 1507 (2021). <https://doi.org/10.3390/nano11061507>
82. A.B. Faia-Torres, M. Charnley, T. Goren, S. Guimond-Lischer, M. Rottmar, K. Maniura-Weber, N.D. Spencer, R.L. Reis, M. Textor, N.M. Neves, *Acta Biomater.* **28**, 64 (2015). <https://doi.org/10.1016/j.actbio.2015.09.028>
83. E.R. Urquia Edreira, A. Hayrapetyan, J.G.C. Wolke, H.J.E. Croes, A. Klymov, J.A. Jansen, J.J.P. van den Beucken, *Biofabrication* **8**, 025006 (2016). <https://doi.org/10.1088/1758-5090/8/2/025006>
84. L. Juignet, B. Charbonnier, V. Dumas, W. Boulefour, M. Thomas, C. Laurent, L. Vico, N. Douard, D. Marchat, L. Malaval, *Acta Biomater.* **53**, 536 (2017). <https://doi.org/10.1016/j.actbio.2017.02.037>
85. C. Yin, Y. Zhang, Q. Cai, B. Li, H. Yang, H. Wang, H. Qi, Y. Zhou, W. Meng, *J. Bone Joint Surg. Am.* **90**, 2485 (2008). <https://doi.org/10.2106/JBJS.G.00499>
86. D. Buser, N. Broggini, M. Wieland, R.K. Schenk, A.J. Denzer, D.L. Cochran, B. Hoffmann, A. Lussi, S.G. Steinemann, *J. Dent. Res.* **83**, 529 (2004). <https://doi.org/10.1177/154405910408300704>
87. D.M. Brunette, *Exp. Cell. Res.* **167**, 203 (1986). [https://doi.org/10.1016/0014-4827\(86\)90217-X](https://doi.org/10.1016/0014-4827(86)90217-X)

88. K.A. Thomas, S.D. Cook, J. Biomed. Mater. Res. **19**, 875 (1985). <https://doi.org/10.1002/jbm.820190802>
89. X.F. Walboomers, H.J. Croes, L.A. Ginsel, J.A. Jansen, J. Biomed. Mater. Res. **47**, 204 (1999). [https://doi.org/10.1002/\(sici\)1097-4636\(199911\)47:2%3c204::aid-jbm10%3e3.0.co;2-h](https://doi.org/10.1002/(sici)1097-4636(199911)47:2%3c204::aid-jbm10%3e3.0.co;2-h)
90. D.M. Brunette, J. Ratkay, B. Chehroudi, Behavior of osteoblasts on micromachined surfaces, in *The Bone Biomaterial Interface*. ed. by J.E. Davies (University of Toronto Press, Toronto, 1991), pp. 170–180
91. Z. Schwartz, C.H. Lohmann, M. Sisk, D.L. Cochran, V.L. Sylvia, J. Simpson, D.D. Dean, B.D. Boyan, Biomaterials **22**, 731 (2001). [https://doi.org/10.1016/s0142-9612\(00\)00241-6](https://doi.org/10.1016/s0142-9612(00)00241-6)
92. K. Anselme, A. Ponche, M. Biggerelle, Proc. Inst. Mech. Eng. H. **224**, 1487 (2010). <https://doi.org/10.1243/09544119JHEIM901>
93. R. Rohanizadeh, S. Atwa, R.S. Mason, A.J. Ruys, P.J. Martin, A. Bendavid, J. Mater. Sci. Mater. Med. **18**, 705 (2007). <https://doi.org/10.1007/s10856-006-0012-2>
94. Russian standard GOST 19807-91. Wrought Titanium and Titanium Alloys. Grades
95. Sandpaper. Coated abrasives. <https://www.sizes.com/tools/sandpaper.htm#Standards>
96. R. Deltombe, K.J. Kubiak, M. Biggerelle, J. Scan. Microsc. **36**, 150 (2014). <https://doi.org/10.1002/sca.21113>
97. D. Nečas, P. Klapetek, Characterization of surface roughness. Presentation at Greifswald, 25 June 2012. <http://gwyddion.net/presentations/talk-roughness-David-Necas-2012.pdf>.
98. M. Biggerelle, D. Najjar, A. Iost, J. Mater. Sci. **38**, 2525 (2003). <https://doi.org/10.1023/A:1023929807546>
99. M. Allen, P. Millett, E. Dawes, N. Rushton, Clin. Mater. **16**, 189 (1994). [https://doi.org/10.1016/0267-6605\(94\)90116-3](https://doi.org/10.1016/0267-6605(94)90116-3)
100. S. Kaja, A.J. Payne, Y. Naumchuk, P. Koulen, Curr. Protoc. Toxicol. **72**, 2.26.1 (2017). <https://doi.org/10.1002/cptx.21>
101. M. Bosetti, M. Santin, A.W. Lloyd, S.P. Denyer, M. Sabbatini, M. Cannas, J. Mater. Sci.: Mater. Med. **18**, 611 (2007). <https://doi.org/10.1007/s10856-007-2309-1>